Mechanistic insight into E22Q-mutation-induced antiparallel-to-parallel β-sheet transition of $A\beta_{16-22}$: An all-atom Simulation study

Xuhua Li[a], Jiangtao Lei[a], Luogang Xie[b], Guanghong Wei[a]*

[a]State Key Laboratory of Surface Physics, Key Laboratory for Computational Physical Sciences (Ministry of Education), and Department of Physics, Fudan University, 2005 Songhu Road, Shanghai, 200438, China

[b]School of Physics and Electronic Engineering, Zhengzhou University Of Light Industry, No.5 Dongfeng Road, Henan, 450002, China

*Corresponding author: Guanghong Wei, E-mail: ghwei@fudan.edu.cn.

This supporting material contains the convergence check of REMD simulations, one supplemental table (Tab. S1) and seven supplemental figures (Figs. S1-S9).

Convergence analysis of REMD simulations

Before analyzing the REMD simulation data, we first checked the sampling efficiency by following the time evolution of temperature swapping of a representative replica in temperature space. As show in Fig. S3 (A) and Fig. S4 (A), the representative replicas visited sufficiently the whole temperature space during the 350 ns REMD simulation for $A\beta_{16-22}$ octamer and its E22Q mutant octamer, demonstrating the representative replicas were not trapped in one single temperature. Other replicas show similar sampling behaviour (data not shown). The convergence of the two REMD simulations was also examined by comparing the follow several parameters within two time intervals using the 250-300 ns and 300-350 ns data of $A\beta_{16-22}$ octamer and $A\beta_{16-22}$E22Q octamer. Those parameters include the dominant secondary structure (coil, β-sheet, β-bridge, bend) probability content of each amino acid and the probability density function (PDF) of radius of gyration (Rg), hydrogen bond (H-bond) number and end-to-end distance of a peptide chain. The secondary structure contents for each residue within the two time intervals of the two systems present a relatively good agreement for each system (Fig. S3, S4). The distributions of Rg, H-bond number and the end-to-end distance of the systems within the two time intervals have large overlaps for both systems (Fig. S3, S4). Taken together, these results provide strong evidence that the $A\beta_{16-22}$ and $A\beta_{16-22}$E22Q octamer systems were reasonably converged within 250 ns.

One supplemental table

Tab. S1. Temperature (K) list used in the 48-replica REMD simulations of both Aβ16-22 and Aβ16-22E22Q octamers.

309.00	310.94	312.90	314.87	316.84	318.82	320.81	322.81
324.82	326.84	328.86	330.90	332.94	335.00	337.06	339.14
341.22	343.32	345.42	347.54	349.66	351.79	353.94	356.09
358.25	360.43	362.61	364.81	367.01	369.23	371.45	373.69
375.93	378.19	380.46	382.74	385.03	387.33	389.64	391.96
394.29	396.65	399.01	401.37	403.75	406.14	408.54	410.95

Seven supplemental figures

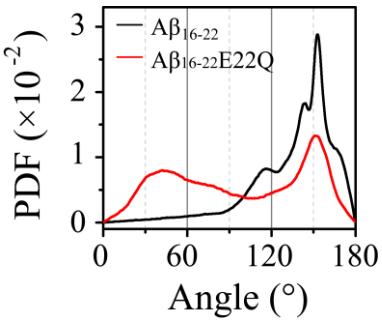

Fig. S1. The PDF of the angle between the two chains of Aβ16-22 and Aβ16-22E22Q dimers.

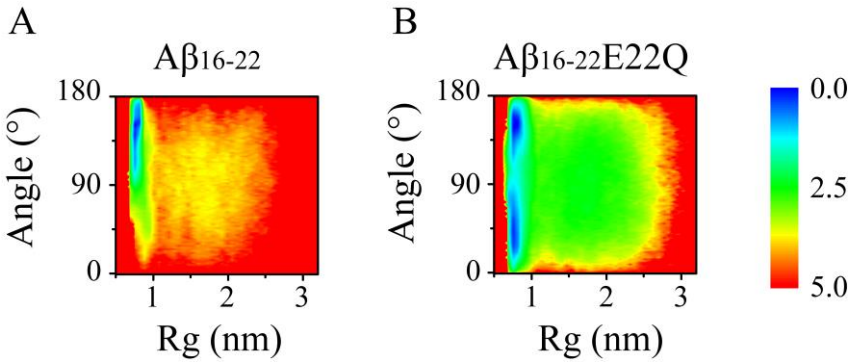

Fig. S2. The free energy landscapes (or PMF) as a function of the Rg and the angle between the two chains of Aβ16-22 (A) and Aβ16-22E22Q (B) dimer systems.

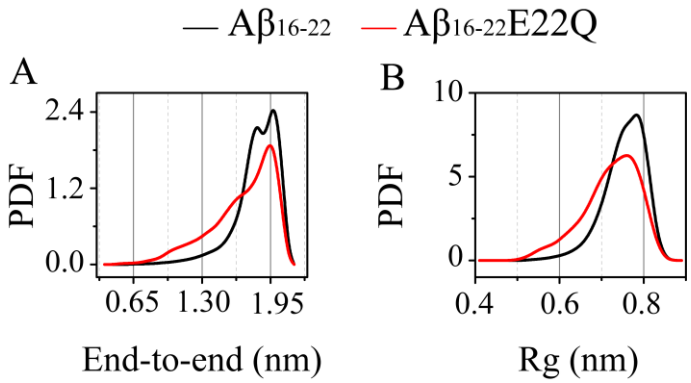

Fig. S3 The PDFs of end-to-end distance (A) and Rg (B) of $A\beta_{16-22}$ and $A\beta_{16-22}$E22Q monomers.

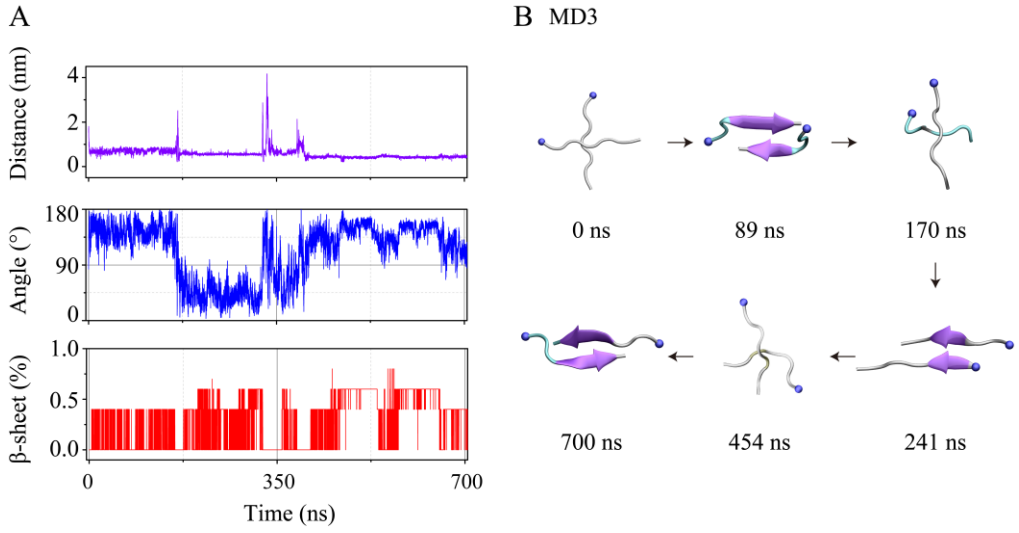

Fig. S4 The assembly process of $A\beta_{16-22}$E22Q dimer system was analyzed using the time evolution of the following three parameters: the inter-molecular F19-F19 minimum distance, the angles between the two chains, and the β-sheet probability (A). The representative snapshots in MD3 of $A\beta_{16-22}$E22Q dimer system. The blue balls represent the N-terminal Cα atom of each chain (B).

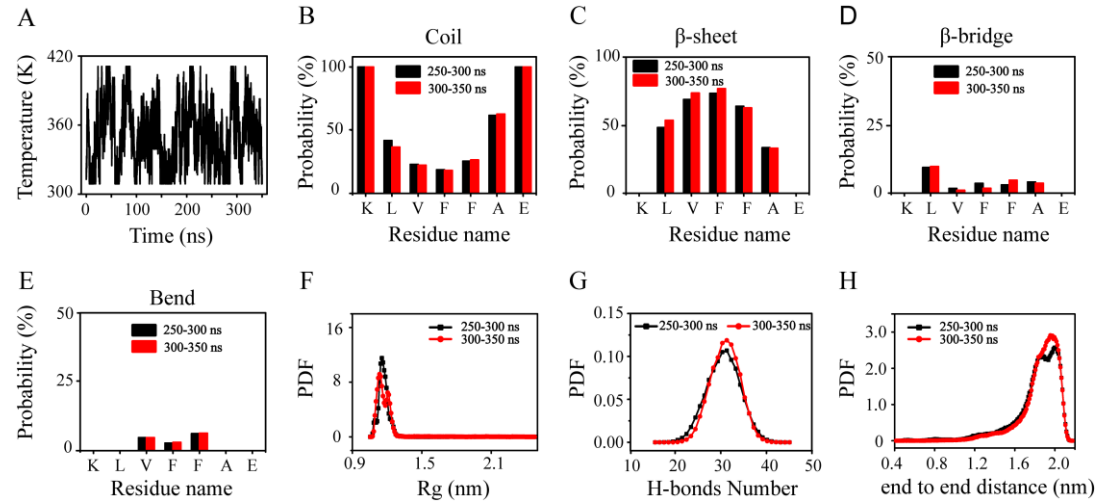

Fig. S5. Simulation convergence assessments for $A\beta_{16-22}$ octamer system using the data generated within 250-300 and 300-350 ns time intervals. We used the following several parameters to check the convergence of the simulation: (A) the time evolution of temperature swapping of one representative replica in temperature space. (B)-(H) the secondary structure propensity of each residue; the probability density function (PDF) of Rg (F), total H-bond number (G) and end-to-end distance (H).

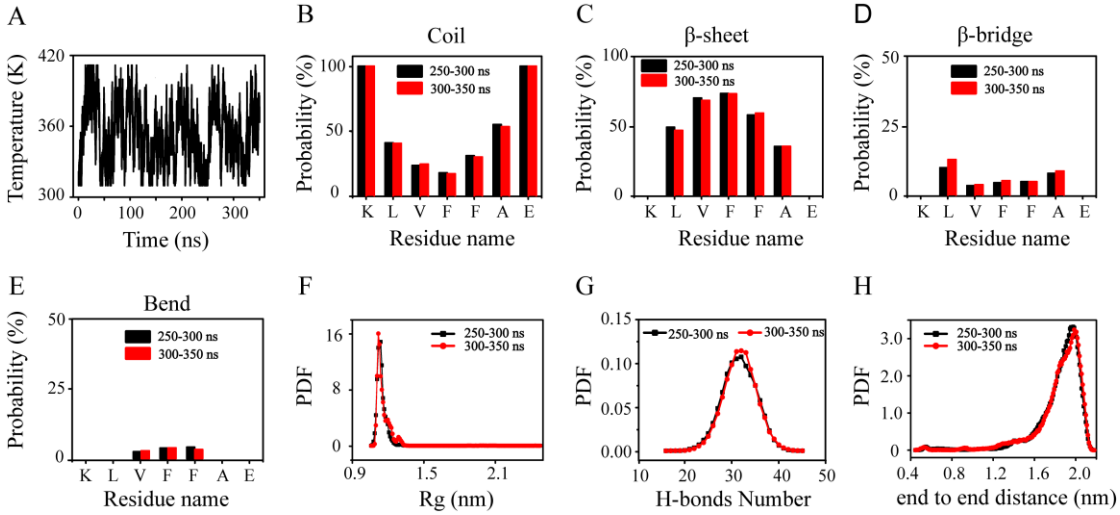

Fig. S6. Simulation convergence assessments for $A\beta_{16-22}$E22Q octamer system using the data generated within 250-300 and 300-350 ns time intervals. We used the following several parameters to check the convergence of the simulation: (A) the time evolution of temperature swapping of one representative replica in temperature space. (B)-(H) the secondary structure propensity of each residue; the probability density function (PDF) of Rg (F), total H-bond number (G) and end-to-end distance (H).

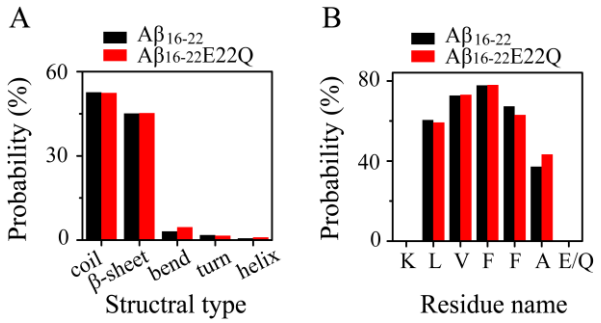

Fig. S7. The comparison of secondary structure between the $A\beta_{16-22}$ and $A\beta_{16-22}E22Q$ octamers. (A) The overall probability of each type of secondary structure. (B) Residue-based β-sheet (include β-sheet and β-bridge) probabilities.

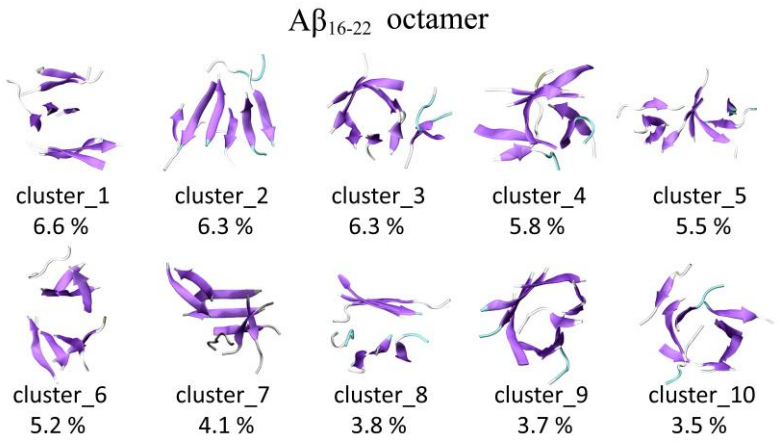

Fig. S8. Representative conformations of the top ten most-populated cluster of $A\beta_{16-22}$ octamer, including single-layered (cluster_2), bilayered (cluster_6 and cluster_8) and trilayered (cluster_1) β-sheets, β-barrel-like (cluster_3) and disordered (cluster_4, cluster_5, cluster_7, cluster_9 and cluster_10) structures.

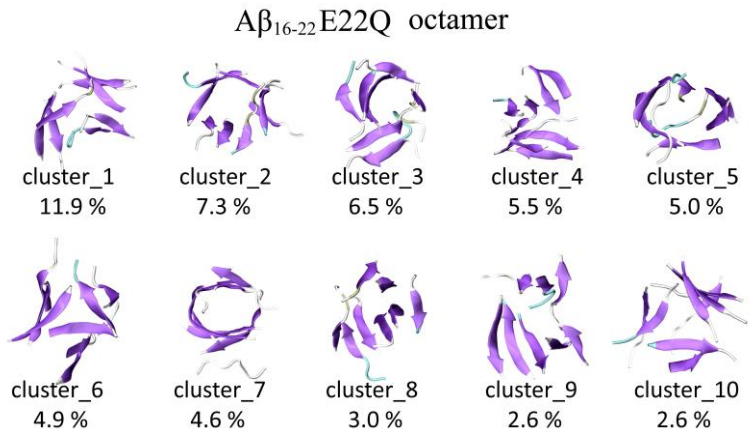

Fig. S9. Representative conformations of the top ten most-populated cluster of $A\beta_{16-22}E22Q$ octamer, including bilayered β-sheets (cluster_8 and cluster_9), β-barrel-like structures (cluster_2 and cluster_7), triangular β-sheets (cluster_6 and cluster_10) and disordered structures (cluster_1, cluster_3, cluster_4, and cluster_5).